Study of Osteogenic Potential of Electrospun PCL incorporated by Dendrimerized Superparamagnetic Nanoparticles as a Bone Tissue Engineering Scaffold

Mahsa Khalili[1], Hamid Keshvari[1], Rana Imani[1], Alireza Naderi Sohi[2], elaheh esmaeili[3], and Maryam Tajabadi[4]

[1]Amirkabir University of Technology
[2]Tarbiat Modares University Faculty of Biological Sciences
[3]Sharif University of Technology
[4]Iran University of Science and Technology

September 14, 2020

Abstract

Nanotechnology plays a promising role in biomedical applications, particularly tissue engineering. Recently, the application of magnetic scaffolds and pulsed electromagnetic field (PEMF) exposure has been considered in bone tissue regeneration. In this study, 3rd generation dendrimer-modified superparamagnetic iron oxide nanoparticles (G3-SPIONs) are synthesized comprehensively characterized. Magnetic polycaprolactone (PCL) nanofibers are prepared by incorporating G3-SPIONs within the electrospinning process ,and physicochemical characteristics ,as well as cytocompatibility and cell attachment are assessed. Eventually, the osteogenic differentiation ability of adipocyte-derived mesenchymal stem cells (ADMSCs) cultured on the magnetic scaffold with and without PEMF exposure was investigated by measurement of alkaline phosphatase (ALP) activity and calcium content. The expression of specific bone markers was studied using the Real-time PCR method. According to the results, G3-SPIONs with mean size and zeta potential of 17.95 ± 3.57 nm and 22.7 mV, respectively, show a high saturation magnetization (57.75 emu/g). Adding G3-SPIONs to PCL significantly decrease nanofibers size to 495±144 nm and improves cell attachment and growth. The ADMSCs cultured on the G3-SPION-PCL scaffold in the presence of osteogenic media (OM) and exposure to PEMF expressed the highest Osteocalcin and Runx2 and showed higher calcium content as well as ALP activity. It can be concluded that the synthesized G3-SPION incorporated PCL nanofibers serve as a promising magnetic scaffold for bone regeneration. Also, utilizing the magnetic scaffold in the presence of OM and PEMF provides a synergistic effect toward osteogenic differentiation of ADMSCs. Key Words: Superparamagnetic iron oxide nanoparticles, Dendrimer, Polycaprolactone, Pulsed electromagnetic field, Bone tissue engineering

Abstract

Nanotechnology plays a promising role in biomedical applications, particularly tissue engineering. Recently, the application of magnetic scaffolds and pulsed electromagnetic field (PEMF) exposure has been considered in bone tissue regeneration. In this study, 3rd generation dendrimer-modified superparamagnetic iron oxide nanoparticles (G3-SPIONs) are synthesized comprehensively characterized. Magnetic polycaprolactone (PCL) nanofibers are prepared by incorporating G3-SPIONs within the electrospinning process ,and physicochemical characteristics ,as well as cytocompatibility and cell attachment are assessed. Eventually, the osteogenic differentiation ability of adipocyte-derived mesenchymal stem cells (ADMSCs) cultured on the magnetic scaffold with and without PEMF exposure was investigated by measurement of alkaline phosphatase (ALP) activity and calcium content. The expression of specific bone markers was studied using the Real-time PCR method. According to the results, G3-SPIONs with mean size and zeta potential of 17.95 ±

3.57 nm and 22.7 mV, respectively, show a high saturation magnetization (57.75 emu/g). Adding G3-SPIONs to PCL significantly decrease nanofibers size to 495±144 nm and improves cell attachment and growth. The ADMSCs cultured on the G3-SPION-PCL scaffold in the presence of osteogenic media (OM) and exposure to PEMF expressed the highest Osteocalcin and Runx2 and showed higher calcium content as well as ALP activity. It can be concluded that the synthesized G3-SPION incorporated PCL nanofibers serve as a promising magnetic scaffold for bone regeneration. Also, utilizing the magnetic scaffold in the presence of OM and PEMF provides a synergistic effect toward osteogenic differentiation of ADMSCs.

Key Words: Superparamagnetic iron oxide nanoparticles, Dendrimer, Polycaprolactone, Pulsed electromagnetic field, Bone tissue engineering

Introduction

According to the American academy of orthopedic surgeons, there are 6.3 million fractures every year in the United States. Although surgery serves as a common treatment for bone fracture, in some cases (around 10%), infection and insufficient vascularization following the may result in incomplete healing (Ng, Spiller, Bernhard, & Vunjak-Novakovic, 2017; Stevens, Yang, Mohandas, Stucker, & Nguyen, 2008). The factors like aging populations and the high incidence of osteo-degenerative diseases significantly lead to growth in the artificial regeneration of bone tissue as a field of research (Joshi & Grinstaff, 2008). Autologous bone grafting is usually known as the gold standard for the treatment of bone defects. However, there are several disadvantages, including painful procedure, high cost, limited tissue supply, and extended hospitalization (Kohli et al., 2018; Polo-Corrales, Latorre-Esteves, & Ramirez-Vick, 2014). On the other hand, despite the abundance of resources for allograft based bone grafting, it has limited application due to the poor adaptation and the risk of disease transmission (Robbins, Lauryssen, & Songer, 2017; Stevens et al., 2008). In order to overcome such limitations, bone tissue engineering is becoming a promising treatment in which the combination of living cells, engineered scaffolds, and biochemical/biophysical factors can enhance tissue regeneration. Actullay, bone issue engineering ,in association with technologies in fracture stabilization, seems as innovative solutions (Campana et al., 2014).

Recently, it has been documented that in addition to physical stimulations including tensile and compressive stresses, fluid shear stresses, and heat showing a remarkable role in osteogenic differentiation, magnetic stimulations can also considerably improve bone regeneration (Xia et al., 2018). In this regards, magnetic nanoparticles (MNPs) incorporation into the bone tissue engineering scaffolds, with or without a magnetic field exposure, have enormous potential for bone tissue engineering applications (Bock et al., 2010; He et al., 2017). Previous studies have demonstrated that ion exchanging channels on the cell membrane and the corresponded biochemical pathway can be influenced by magnetic fields (Zhao et al., 2011). Magnetic scaffolds in which MNPs are incorporated have significant effects on adhesion, proliferation, and differentiation potency of stem cells. The force generated by magnetic nanoparticles under a magnetic field can significantly influence the micro-environment around the cells, leading to a series of changes in cell behavior via magneto-mechanical stimulations (Jiang et al., 2016; Xia et al., 2019; Xia et al., 2018). Among MNPs, iron oxide nanoparticles have attracted much interest in biomedical applications such as magnetic-activated cell sorting (MACS), hyperthermia, drug delivery, and contrast-enhanced MRI, because they belong to a group of non-toxic materials that exhibit good biocompatibility due to the presence of iron ions (Kandpal, Sah, Loshali, Joshi, & Prasad, 2014) (Chauhan et al., 2013; Ito, Shinkai, Honda, & Kobayashi, 2005). (Ayyappan et al., 2010; Koehler et al., 2009; Marinin, 2012). As a challenging issue, in biological media, MNPs usually tend to be agglomerated because of the high surface-area-to-volume ratio as well as magnetic attraction. To avoid this problem and to stabilize nanoparticles, the MNPs surface coating is preferred (Mascolo, Pei, & Ring, 2013). Ideally, these coatings should be non-immunogenic and hydrophilic enough to prevent the opsonization by plasma proteins resulting decrease in reticuloendothelial system clearance and an increase in the shelf-life within the body. The materials used for coating are commonly polymeric ones with improved physical-chemical properties and appropriate biocompatibility (Chauhan et al., 2013; Favela-Camacho, Samaniego-Benítez, Godínez-García, Avilés-Arellano, & Pérez-Robles, 2019). Dendrimers are highlighted by their unique properties, such as mono-dispersity, well-defined structure, having a large number of surface

functional groups, and antimicrobial activities. Such characteristics make them an appropriate tool for biomedical applications, particularly tissue engineering (Abdel-Sayed et al., 2016; Gorain et al., 2017; Kesharwani, Gajbhiye, K Tekade, & K Jain, 2011; Kesharwani, Tekade, Gajbhiye, Jain, & Jain, 2011; Kesharwani, Tekade, & Jain, 2015). Incorporation of dendrimers into the scaffolds structure, particularly in the surface, may improve cell-substrate interactions. Besides, the dendrimers due to the porous structure could improve the interconnection in the scaffolds structure and consequently help to cell-cell interactions (Gorain et al., 2017; Joshi & Grinstaff, 2008). Poly (amidoamine) dendrimers, PAMAM, have received widespread attention because of the fundamental nature and their polar properties (Bosman, Janssen, & Meijer, 1999). PAMAM are hydrophilic, biocompatible, monodisperse, and cascade-branched macromolecules with highly flexible surface chemistry. In order to reduce MNPs agglomeration and increase their cationic surface charge, coating with PAMAM can be considered as an ideal option because PAMAM has plenty of peripheral functional groups and high hydrophilicity. PAMAM dendrimers can introduce a dense outer amine shell on the MNPs through a cascade-type generation (Boas, Christensen, & Heegaard, 2006; Khodadust, Unsoy, Yalcın, Gunduz, & Gunduz, 2013; Klajnert & Bryszewska, 2001). Polycaprolactone (PCL) is considered as an appropriate candidate for bone tissue engineering regarding its long-term degradation. the FDA approves PCL for some clinical applications. It is biodegradable polyester and appropriate for long-term bone implantation. Studies have shown that PCL act as a supportive role to keep living osteoblasts and fibroblasts cells. PCL maintains its primary structure in the biological fluids and tends to blend with other polymers. [31] Considering the inherent properties of MNPs, positive features of dendrimers as a right candidate for surface coating, this project aimed to synthesize a PCL-based magnetic scaffold by incorporation of dendrimers-modified MNPs. Iron oxide nanoparticles (SPION) were functionalized by 3rd generation of PAMAM dendrimer and comprehensively characterized. Dendrimerized SPIONs were incorporated into the PCL nanofibrous scaffold by blend electrospining. Osteogentic differentiation of MSCs cultured on the magnetic scaffolds was studied in the presence of pulsed electromagnetic field produced by bioreactor.

Materials and methods

2.1. Chemicals

Ferrous chloride hexahydrate ($FeCl_3.6H_2O$), ferric sulfate heptahydrate ($FeSO_4.7H_2O$), (3-aminopropyl) triethoxysilane (APTES), methanol (CH_3OH), ethanol (C_2H_5OH), Chloroform (CHCl3), dimethyl sulfoxide (DMSO) and beta-glycerol phosphate were purchased from Merck (Darmstadt, Germany). Methyl acrylate (MA), ethylenediamine (EDA), ammonium hydroxide (NH_4OH), polycaprolactone (PCL, M_W= 70000-90000 g/mol), dimethylformamide (DMF), 3-[4,5-dimethylthiazol-2-yl]-2,5-diphenyltetrazolium bromide (MTT), dexamethasone, ascorbic acid-2-phosphate, glutaraldehyde, paraformaldehyde, and diarylpyrimidine (DAPI) were purchased from Sigma-Aldrich (St. Louis, MO) and used without further purification. Dulbecco's Modified Eagle's Medium (DMEM), fetal bovine serum (FBS), penicillin/streptomycin were purchased from Gibco (USA). Human adipose mesenchymal stem cells (ADMSCs) obtained from Stem Cells Technology Research Centre cell bank (Tehran, Iran).

2.2. **Synthesis of SPIONs**

The co-precipitation method was used to synthesize SPIONs following the reported standard protocol. (Esmaeili, Khalili, et al., 2019; Tajabadi, Khosroshahi, & Bonakdar, 2013) A solution mixture of ferrous chloride hexahydrate ($FeCl_3.6H_2O$), 0.2 M, and ferric sulfate heptahydrate ($FeSO_4.7H_2O$), 0.1 M, was prepared in distilled water and used as a source of iron ions. The aqueous ammonia solution (5.4 M) was added dropwise to the solution of iron salts under nitrogen protection and stirred at 50 °C for 30 min. The obtained precipitation was washed five times with distilled water using magnetic separation to remove any excess unreacted materials and air-dried at room temperature.

2.3. Synthesis of APTES modified SPIONs

A suspension of SPIONs was prepared with a concentration of 0.5 M in ethanol and sonicated for 30. Then, a 10 ml APTES solution, 10% v/v, was added to the solution and stirred for five h. The final product was purified five times with ethanol by magnetic separation. Then, the obtained APTES modified SPIONs were

dried at room temperature to remove excess solvent.

2.4. Synthesis of dendrimer functionalized SPIONs

PAMAM dendrimer was coated on the surface of APTES modified SPIONs in two steps according to the previous reports with some modification (Liu, Guo, Jin, Yang, & Wang, 2008; Pan et al., 2007; Tajabadi et al., 2013). In the first step, 10 ml of 5% (w/v) APTES modified SPIONs in methanol was sonicated for 20 minutes. Then, 50 ml of 20% (v/v) methyl acrylate was added dropwise to the stirring solution at room temperature for 24 hrs. The resultant solution was washed with methanol five times and separated with a magnetic magnet. In the second step, 10ml of 50% (v/v) ethylenediamine was added to the purified magnetic nanoparticles and stirred for three h and was then placed in the ultrasonic water bath for one h. The final product was sedimented by a magnetic magnet and washed with methanol five times. After completing the second step, a full generation of dendrimers was formed on amine-functionalized magnetic nanoparticles. These steps were repeated two times to achieve the third generation of dendrimer on SPIONs. Fig 1, demonstrates the schematic representation of the synthesis reaction of SPION-G3.

2.5. Fabrication of electrospun PCL scaffolds

The PCL pellets were dissolved in a mixture of chloroform and DMF, as a solvent, with a volume ratio of 80:20 to obtain a final concentration of 12% (w/v). To prepare G3-SPIONs suspension in PCL, 0.1 (w/v) of nanoparticles was added to the PCL solution and sonicated to disperse. The electrospinning process was done at a constant flow rate of 0.3 ml/h and the applied voltage of 20 kV. The distance of the needle to the cylinder collector was set at 20 cm. After that, plasma treatment was done to create surface hydrophilicity using a plasma generator (Diener Electronics, Ebhausen, Germany). Surface treatment was performed with radiofrequency power set at 44 kHz and pure oxygen introduction, 0.4 mbar, for 5 minutes.

2.6. Characterizations

TEM analysis of synthesized SPIONs was performed using an FEI Tecnai G2 Spirit TWIN apparatus. The 1 mg/ml aqueous suspension of G3-SPIONs was placed on the carbon-coated copper grids to evaluate the size and morphology of SPIONs.

The size distribution and the surface charge of magnetic nanoparticles were determined by Zetasizer Nano ZS, Malvern, UK. The synthesized nanoparticles were dispersed in methanol by probe sonication for 10 min and then analyzed by the instrument.

FTIR analysis was used to prove the surface functionalization of SPIONs with APTES and PAMAM dendrimer. For this purpose, a solid powder of nanoparticles was mixed by KBr powder to form a pellet. Infrared spectra profiles were obtained using BOMEM-SRG1100G FTIR spectrophotometer in the range of 400-4000 cm^{-1} in the transmittance mode at room temperature. The magnetic property of the nanoparticles was evaluated by the Vibrating sample magnetometer (VSM-par155). This assessment was carried out at room temperature under the applied magnetic field of 8 kOe. To evaluate the morphological cues and microstructure of the electrospun nanofibers, the samples were coated with a thin layer of gold using a sputtering machine (Emitech K450X, Ashford, UK). Then, images were observed by scanning electron microscope (AIS2100; Seron Technology, Uiwang-si, Gyeonggi-do, South Korea) with 15 kV accelerating voltage. The mean diameter and standard deviation of the nanofibers were assessed by the image analyzer.

2.7. Cell culture studies

2.7.1. MTT assay

MTT assay was used to study the proliferation potential and survival of adipose-derived mesenchymal stem cells (ADMSCs) on different substrates. After plasma processing, scaffolds were cut into disks (11 mm diameter) and sterilized with 70% ethanol and ultraviolet light exposure (40 minutes and 120000 µ J/CM2). After being placed in the culture medium overnight, the cells were seeded on the samples at a density of 5×10^3 cells/sample, and then incubated in 5% CO_2 at 37 °C in high glucose Dulbecco's modified Eagle's medium, DMEM, supplemented with 10% fetal bovine serum, FBS, and 1% penicillin-streptomycin. The

cytotoxicity value of the prepared scaffold (PCL and G3-SPION-PCL) was evaluated using MTT assay on days 1, 3, 7, and 14 after the seeding of ADMSCs cells and compared to the tissue culture plates (TCP), as control. The samples were washed with PBS and incubated in 10% V/V MTT in a DMEM solution at 37 °C for three h. (Esmaeili, Soleimani, et al., 2019) After the formation of the formazan crystals inside the cells seeded on the scaffolds, Then, the supernatant was removed, DMSO was added to dissolve the Formosan crystals, and the absorbance of the purple solution was measured at 570 nm in a microplate reader (BioTek, ELX800, USA).

2.7.2. DAPI staining

In order to study the cell adhesion on the scaffolds on days 1 and 14, the nucleus staining of the cells using DAPI was implemented. Cells were fixed with 4% paraformaldehyde and kept at 4@C for 20 minutes and at room temperature for 5 minutes. The samples were subsequently washed with PBS and stained with DAPI solution for 1 minute in a dark place. Following the washing, three times, by PBS, the samples were imaged using a fluorescent microscope (Nikon, Tokyo, Japan).

2.7.4. Scanning electron microscopy (SEM)

For studying growth morphology using SEM, the samples were washed and fixed in 2.5% glutaraldehyde for two h at room temperature. Then, the samples dehydrated by incubating in ethanol for ten min ,which the concentration is gradually increased (50, 60, 70, 80, 90, and 100% V/V). Finally, the dehydrated samples were dried and sputter-coated with gold and visualized using SEM.

2.7.5. Cell differentiation

ADMSCs differentiation cultured on the magnetic scaffold to osteoblast cells was studied under the osteogenic medium, OM, 250 nM dexamethasone, ten mM beta-glycerol phosphate and 50 µg/ml ascorbic acid-2-phosphate, DMEM, 10% FBS, 1% penicillin/streptomycin and low frequency pulsed electromagnetic fields, PEMF, 30 mT ,and 75 Hz, eight h/day.

The osteogenic differentiation of ADMSCs was assessed in different conditions in 5 groups, the cells seeded on TCP, PCL, and G3-SPION-PCL under OM, and the cells seeded on G3-SPION-PCL under PEMF, with and without OM. The cells were under PEMF for 14 days ,and 8 hours per day and OM was changed every other day for 14 days.

2.7.6. Calcium assay

The calcium content assay is a direct colorimetric assay based on the O-Cresolphtalein method (Baldino et al., 2015). The samples were washed with PBS and lysed by 0.6 M HCL. After addition of the reagent to the calcium solutions, based on the applied kit protocol (Pars Azmoon, Iran), the optical density (OD) of the samples was measured at 570 nm.

2.7.7. Alkaline phosphatase activity assay

ALP activity, as an early osteogenic marker, is used on days 7 and 14 to evaluate the osteogenic differentiation. The samples were washed with PBS and were lysed by RIPA buffer to measure the total protein and ALP activity. Based on the ALP activity kit (Pars Azmoon, Iran), after addition of the reagent, the optical density of the samples was measured at 405 nm and normalized against the total protein (BCA kit, Thermo Scientific).

2.7.8. Real-time polymerase chain reaction (RT-PCR) assay

RT-PCR was used to study the effect of prepared scaffolds and PEMF on the osteogenic gene expression ,including collagen type 1 (Col1), Runt-related transcription factor 2 (Runx2), and Osteocalcin (OC). At first, total mRNA was extracted using Qiazol reagent after 14 days of culturing MSCs. Afterward, cDNA was synthesized by MLV reverse transcriptase (RT) ,and random hexamer according to the manufacturer's instructions (Fermentas). The rate of gene expression was quantified by an RT-PCR analyzer (Corbett, Australia) and Rotor-Gene software was used to quantify the gene expression level. In this study, the

expression of the target gene was evaluated via the relative quantification model compared to β2M control as a housekeeping gene. Relative gene expression was calculated by [?][?]Ct method. The primer sequences of corresponding genes are presented in Table 1.

Results and Discussion

In this study, we synthesized iron oxide nanoparticles showing superparamagnetic properties. These nanoparticles highly tend to aggregate ,which increases the overall size of the nanoparticles and consequently precipitate them. Thus, surface modification seems necessary to stabilize SPIONs and improve their biocompatibility (Gupta & Gupta, 2005; Hamley, 2003; Ito et al., 2005). PAMAM dendrimer was chosen as an appropriate surface modification because of its high water solubility, biocompatibility, antimicrobial properties, and positively charged amine groups (Chawla, Shetty, Goyal, Rathore, & Sharma, 2018; Fox, Richardson, & Briscoe, 2018).

The size and morphology of G3-SPIONs have been analyzed using the TEM instrument and shown in Fig. 2a. The prepared G3-SPIONs had spherical shape with the uniform size distribution. The average diameter of nanoparticles was measured by the ImageJ software (NIH, Bethesda, MD) and estimated to be 17.95 ± 3.57 nm. The three-dimensional structure of dendrimers endues SPIONs steric stabilization, and thus well-dispersity (Yen, Lien, Chung, & Yeh, 2017).

G3-SPIONs were also characterized by DLS ,which measures the hydrodynamic diameter of the MNPs in their dispersion state (Fig. 2b). The result showed that the average size of the nanoparticles was 28.91 nm ,which as expected, was more significant than the size obtained by transmission electron microscopy (Souza, Ciminelli, & Mohallem, 2016). The surface charge of G3-SPIONs ,which is a crucial parameter for the electrostatic interaction between cells and the surface of the material was assessed by zeta potential measurement. The zeta potential of G3-SPIONs was 22.7 mV due to amine groups in PAMAM dendrimer with a positive charge (Fig. 2c). Since some of G3-SPIONs may be exposed on the nanofiber surface, the positive charge can increase the cell attachment on the scaffold's surface and consequently improve cell-substrate interactions.

SPIONs functionalization and coating by APTES and PAMAM dendrimers, respectively, on the surface of SPIONs were approved by FT-IR spectroscopy, as shown in Fig. 3a. The characteristic absorption band at 586 cm^{-1} is attributed to the stretching bond of the Fe–O which confirms the presence of Fe_3O_4 nanoparticles. The peak at 1021 cm^{-1} is assigned to the stretching vibration of the Si-O-Fe bond, proving the presence of SiO_2 shell on the surface of SPIONs. The peaks around 2866 cm^{-1} and 2912 cm^{-1} are due to the existence of stretching vibration of CH_2 in the aminopropyl group which confirms the binding of APTES molecules. The broad peak at 3430 cm^{-1} is due to the stretching mode of the NH_2 group and the band at 1634 cm^{-1}exhibits a stretching vibration of –CO–NH– group, representing the binding of PAMAM dendrimers on the surface of SPIONs. It can be observed that increasing the order of PAMAM generation increases the intensity of these peaks.

The magnetization property of SPIONs ,and G3-SPIONs was measured using VSM at room temperature . As shown in Fig. 3b, the negligible remanence (M_r) and zero coercivity (H_C) of the magnetic nanoparticle confirm the superparamagnetic behavior of the samples ,which prevents the formation of a stable magnetic state and enables them to re-disperse rapidly in ,the absence of magnetic field. compared with the maximum magnetization (M_S) value of 68.28 emu/g for SPIONs, the M_s value for G3-SPIONs decreases to 57.75 emu/g due to the linkage of non-magnetic PAMAM dendrimer on ,the surface of SPIONs. Non- magnetic layer of PAMAM inevitably lead to an unavoidable decrease in saturation magnetization. It can result from a decrease in the strength of the exchange interaction between oxygen and iron atoms (Uzun et al., 2010). According to Taghavi et al., the VSM result of bare MNPs analyzed at 37 [?]C was obtained as 48.8 emu/g (POURIANAZAR, 2016) Zhu et al. have prepared Poly peptide dendrimers through the ligand-exchange method synthesized on MNPs. The saturation magnetization for G3(Lysine) and G3(Glutamine) were reported 42.9 and 41.6, respectively. According to recent studies, the saturation magnetization is related to the particle size, directly. The reason for the decrease in saturation magnetization arises from the

increase in non-magnetic surface coverage of each particle G3(Lys) and G3(Glu) as ligand-exchange (Zhu et al., 2011). Considering the mentioned studies, it could be concluded that the saturation magnetization value of the SPION and G3-SPION is comparable with that obtained in the previous studies.

The G3-SPIONs was embedded into the PCL nanofibers to be used as a scaffold in the osteogenesis differentiation. The SEM micrographs of PCL and G3-SPION-PCL nanofibrous scaffolds are presented in Fig. 4, to analyze the diameter and morphology of the prepared scaffold. As shown, the nanofibrous scaffolds have a cylindrical shape without any structural imperfection resulting from the proper selection of electrospinning parameters. The average fiber diameter of the PCL and G3-SPION-PCL nanofibers obtained 866+-310 and 495+-144, respectively. It was observed that the presence of G3-SPIONs in the scaffold has reduced the size and distribution of fiber diameter ,which is justifiable by higher conductivity of the polymer solution in the presence of G3-SPIONs. High porosity and nanostructure property of the scaffolds endue a high potential for cell attachment ,which can be used in tissue engineering. Although the suitable average diameter of electrospun PCL nanofibers for bone tissue engineering was reported in the wide range, from 20 to 5000 nm, the average fiber diameter of the prepared nanocomposite fibers was in the range of bone tissue engineering applications, as confirmed by other studies (Jang, Castano, & Kim, 2009; Ren, Wang, Sun, Yue, & Zhang, 2017).

The MTT assay was used to investigate the proliferation rate and viability of ADMSCs on electrospun PCL and G3-SPION-PCL scaffolds on days 1, 3, 7, and 14. As shown in Fig. 5a, cell growth, and proliferation have an increasing trend for all groups, indicating the biosafety of the prepared scaffolds. As can be observed, there was no statistically significant difference between the OD value of the cells cultured on the PCL and G3-SPION-PCL on day 1. However, the difference has been increased until the significant discrepancy has been observed on day 14, indicating a higher rate of proliferation and growth on G3-SPION-PCL compared with PCL scaffold. The better cell growth on G3-SPION-PCL can be attributed to G3-SPIONs nanoparticles ,which endue more hydrophilicity and positive surface charge to the prepared scaffold, leading to the improved cell growth and proliferation. It is noticeable that the porous structure of the scaffolds causes the migration of some seeded cells from the porous nanofibrous scaffold to the TCP plate, resulting in lower OD value of the scaffolds compared with TCP.

The potential of PCL and G3-SPION-PCL nanofibrous scaffolds on cell attachment and ADMSCs proliferation rate was also evaluated by DAPI staining on days 1 and 14. As shown in Fig. 5b, the scaffold containing G3-SPIONs showed enhanced cell attachment ,and growth compared to the neat scaffold, PCL. The MTT assay indicated that the G3-SPION-PCL scaffold was more compatible than PCL and according to the images of DAPI staining the number of attached cells to G3-SPION-PCL was much more than PCL. It can be concluded that the presence of G3-SPIONs decreases the fiber diameter, increases the surface to volume ratio,and affect significantly on the cell attachment. Overall, surface topography, hydrophilicity, and positively charged PAMAM dendrimers ,which were partially exposed on the scaffold surface play a vital role in the interaction of cells to the scaffold (Gloria et al., 2013).

An electromagnetic bioreactor was used to induced EMF and enhance the osteogenesis of ADMSCs mediated by incorporated SPIONs. Many studies demonstrated that EMF has a positive effect on the osteoblast and adipocyte differentiation of mesenchymal stem cells (Wang, Wu, Yang, & Song, 2016). Possible effects of scaffold modification via incorporation of the dendrimerized SPIONs, in the presence of biochemical (OM), and biophysical signaling factors (PEMF) on osteogenesis potential of ADMSCs was evaluated by monitoring the expression of the osteogenic marker on days 7 and 14 after cell seeding.

ALP activity is known as an early marker of osteogenic differentiation. The research studies have indicated that the ALP enzyme plays an essential role in the initiation of mineralization (Miron & Zhang, 2012). As shown in Fig. 6a, the presence of SPIONs, OM, and PEMF resulted in a significant difference in ALP activity between G3-SPION-PCL/OM/PEMF and the other group. The presence of both biochemical and biophysical factors increased the ALP activity ,which is in line with the previous studies reported on the positive effect of electromagnetic waves on the osteogenic differentiation (Xia et al., 2018). Dankova et al. (Daňková et al., 2015) demonstrated that the PCL-MNPs scaffolds increased the ALP activity significantly

in cells cultivated on the PCL-MNPs on day 7 (OD around 0.2). Here, higher ALP activity could be due to dendrimers coated MNPs, which significantly promote adhesion density and osteoblast proliferation via 3D structure and considerable positive charge. The calcium deposition value, as the late marker of osteogenic differentiation, was evaluated quantitatively by calcium content assay, Fig. 6b. As shown, there were no significant differences between the amount of calcium deposition in TCP and PCL scaffold. While the calcium content of G3-SPION-PCL/OM, G3-SPION-PCL/PEMF, and G3-SPION-PCL/OM/PEMF is significantly higher than TCP and PCL. Also, G3-SPION-PCL/OM/PEMF significantly showed higher calcium content than the other groups, confirming the synergistic effect of OM and PEMF in the osteogenic differentiation of ADMSCs. Since the G3-SPION-PCL/OM/PEMF group demonstrated the best ALP activity ,as well as calcium deposition in the osteogenic differentiation, SEM analysis of this sample was performed to investigate the cell adhesion, morphological features, , and shape of the cells on days 1 and 14. As shown in Fig. 6c, no calcium precipitation was observed on the first day, but upon differentiation on day 14 led to a higher level of calcium deposition. Dendritic architecture introduced benefits over linear polymers with the aim of in vitro bone cell growth and adhesion (Joshi & Grinstaff, 2008). Also, it was observed that the morphology of hMSCs showed a significant change from a fibroblastic shape into a polygonal shape during osteodifferentiation (Erices, Conget, Rojas, & Minguell, 2002). This study confirms that the rational design of dendritic architectures can result in the fabrication of new scaffolds with improved properties**.** The effect of PEMF and OM on the expression level of osteogenic transcription factors was evaluated on day 14. As shown in Fig. 7, the ADMSCs seeded on the G3-SPION-PCL scaffold in the presence of OM and exposure to PEMF expressed the highest level of Osteocalcin and Runx2. Osteocalcin, as the most plentiful non-collagenous bone matrix protein, is mainly expressed by osteoblasts and serves a specific marker for the late stages of bone differentiation. Whenever Osteocalcin is overexpressed, the mineral species maturation will be accelerated and modulates osteogenic differentiation of MSCs (Tsao et al., 2017). The superposition of OM and PEMF resulted in significant expression of this gene by ADMSC cultured on the G3-SPION-PCL scaffold.

Collagen type I (Col 1) is an early marker of bone differentiation and the most abundant protein in the bone matrix. The result (Fig. 7) demonstrated overexpression of Col 1 by the cells cultured on the G3-SPION-PCL scaffold under the only PEMF exposure. Interestingly, this result showed that PEMF exposure accelerates early-stage osteogenic differentiation. However, in the combination with OM and PEMF exposure, Col 1 expression did not show such elevation. Recent researches have proved that PEMFs improve osteogenic differentiation of MSCs by stimulating the mRNAs expression of osteogenic related genes such as RunX2, ALP, and BMP2 (Chen et al., 2019). Taking together, it could be concluded that the presence of G3-SPIONs in the PCL scaffold along with simultaneously PEMF exposure and OM increases the differentiation rate of ADMSCs to osteogenic linage and can be a suitable candidate in bone tissue engineering.

Conclusion

In this study, SPIONs were synthesized by the co-precipitation method and modified by G3-PAMAM dendrimer using a divergent method. The nanoparticles were incorporated into the PCL scaffold by electrospinning to produce a novel magnetic scaffold. The influence of G3-SPIONs incorporation on the properties of the magnetic electrospun nanofibers were investigated. MTT assay and DAPI staining confirmed enhancement in growth and proliferation of stem cells seeded on magnetic G3-SPION-PCL compared to the pure PCL. After that, the osteogenic differentiation of the magnetic electrospun scaffolds under biochemical (OM) and biophysical (PEMF) stimulations were investigated ,and analyzed by calcium content assay, ALP activity and real-time PCR. Results interestingly confirmed the superposition effect of G3-SPIONs and PEMF to increase osteogenic differentiation of ADMSCs.

In conclusion, this study suggests that G3-SPION incorporated PCL nanofibers could be considered as a potential magnetic scaffold for bone tissue regeneration applications.

Acknowledgments

The author would like to appreciate the scientific help and guidance of Ms. Simzar Hosseinzadeh. Also,

authores declar no conflict of interest.

Funding

This research did not receive any specific grant from funding agencies in the public, commercial, or not- for-profit sectors.

References

Abdel-Sayed, P., Kaeppeli, A., Siriwardena, T., Darbre, T., Perron, K., Jafari, P., . . . Applegate, L. A. (2016). Anti-microbial dendrimers against multidrug-resistant P. aeruginosa enhance the angiogenic effect of biological burn-wound bandages. *Scientific reports, 6* , 22020.

Ayyappan, S., Mahadevan, S., Chandramohan, P., Srinivasan, M., Philip, J., & Raj, B. (2010). Influence of Co2+ ion concentration on the size, magnetic properties, and purity of CoFe2O4 spinel ferrite nanoparticles. *The Journal of Physical Chemistry C, 114* (14), 6334-6341.

Baldino, L., Sarno, M., Cardea, S., Irusta, S., Ciambelli, P., Santamaria, J., & Reverchon, E. (2015). Formation of cellulose acetate–graphene oxide nanocomposites by supercritical CO2 assisted phase inversion. *Industrial & Engineering Chemistry Research, 54* (33), 8147-8156.

Boas, U., Christensen, J., & Heegaard, P. M. (2006). Dendrimers: design, synthesis and chemical properties. *Journal of Materials Chemistry, 16* (38), 3785-3798.

Bock, N., Riminucci, A., Dionigi, C., Russo, A., Tampieri, A., Landi, E., . . . Dediu, V. (2010). A novel route in bone tissue engineering: magnetic biomimetic scaffolds.*Acta biomaterialia, 6* (3), 786-796.

Bosman, d. A., Janssen, H., & Meijer, E. (1999). About dendrimers: structure, physical properties, and applications. *Chemical reviews, 99* (7), 1665-1688.

Campana, V., Milano, G., Pagano, E., Barba, M., Cicione, C., Salonna, G., . . . Logroscino, G. (2014). Bone substitutes in orthopaedic surgery: from basic science to clinical practice. *Journal of Materials Science: Materials in Medicine, 25* (10), 2445-2461.

Chauhan, R. P., Mathur, R., Singh, G., Kaul, A., Bag, N., Singh, S., . . . Mishra, A. K. (2013). Evaluation of Folate Conjugated Superparamagnetic Iron Oxide Nanoparticles for Scintigraphic/Magnetic Resonance Imaging. *Journal of biomedical nanotechnology, 9* (3), 323-334.

Chawla, R., Shetty, K., Goyal, M., Rathore, A., & Sharma, A. (2018). Medicine Soaring with Nanofever.*J Nanosci Curr Res, 3* (220), 2572-0813.1000220.

Chen, L., Peng, J., Zhao, J., Long, Y., Xie, Y., & Nie, J. (2019). Magnetic Materials in Promoting Bone Regeneration. *Frontiers in Materials, 6* , 268.

Daňková, J., Buzgo, M., Vejpravova, J., Kubíčková, S., Sovková, V., Vysloužilová, L., . . . Amler, E. (2015). Highly efficient mesenchymal stem cell proliferation on poly-ε-caprolactone nanofibers with embedded magnetic nanoparticles.*International journal of nanomedicine, 10* , 7307.

Erices, A., Conget, P., Rojas, C., & Minguell, J. J. (2002). Gp130 activation by soluble interleukin-6 receptor/interleukin-6 enhances osteoblastic differentiation of human bone marrow-derived mesenchymal stem cells. *Experimental cell research, 280* (1), 24-32.

Esmaeili, E., Khalili, M., Sohi, A. N., Hosseinzadeh, S., Taheri, B., & Soleimani, M. (2019). Dendrimer functionalized magnetic nanoparticles as a promising platform for localized hyperthermia and magnetic resonance imaging diagnosis.*Journal of cellular physiology, 234* (8), 12615-12624.

Esmaeili, E., Soleimani, M., Ghiass, M. A., Hatamie, S., Vakilian, S., Zomorrod, M. S., . . . Hosseinzadeh, S. (2019). Magnetoelectric nanocomposite scaffold for high yield differentiation of mesenchymal stem cells to neural-like cells.*Journal of cellular physiology, 234* (8), 13617-13628.

Favela-Camacho, S. E., Samaniego-Benítez, E. J., Godínez-García, A., Avilés-Arellano, L. M., & Pérez-Robles, J. F. (2019). How to decrease the agglomeration of magnetite nanoparticles and increase their stability using surface properties. *Colloids and Surfaces A: Physicochemical and Engineering Aspects, 574* , 29-35.

Fox, L. J., Richardson, R. M., & Briscoe, W. H. (2018). PAMAM dendrimer-cell membrane interactions.*Advances in colloid and interface science* .

Gloria, A., Russo, T., D'Amora, U., Zeppetelli, S., D'Alessandro, T., Sandri, M., . . . Tampieri, A. (2013). Magnetic poly (ε-caprolactone)/iron-doped hydroxyapatite nanocomposite substrates for advanced bone tissue engineering. *Journal of the Royal Society Interface, 10* (80), 20120833.

Gorain, B., Tekade, M., Kesharwani, P., Iyer, A. K., Kalia, K., & Tekade, R. K. (2017). The use of nanoscaffolds and dendrimers in tissue engineering. *Drug Discovery Today, 22* (4), 652-664.

Gupta, A. K., & Gupta, M. (2005). Synthesis and surface engineering of iron oxide nanoparticles for biomedical applications. *Biomaterials, 26* (18), 3995-4021.

Hamley, I. (2003). Nanotechnology with soft materials. *Angewandte Chemie International Edition, 42* (15), 1692-1712.

He, J., Hu, H., Zeng, X., Lan, F., Wu, F., & Wu, Y. (2017). A magnetic hydroxyapatite composite scaffold-based magnetic therapy for bone repair: an experimental study in canis lupus familiaris. *Regenerative Biomaterials, 4* (2), 97-103.

Ito, A., Shinkai, M., Honda, H., & Kobayashi, T. (2005). Medical application of functionalized magnetic nanoparticles. *Journal of bioscience and bioengineering, 100* (1), 1-11.

Jang, J.-H., Castano, O., & Kim, H.-W. (2009). Electrospun materials as potential platforms for bone tissue engineering. *Advanced drug delivery reviews, 61* (12), 1065-1083.

Jiang, P., Zhang, Y., Zhu, C., Zhang, W., Mao, Z., & Gao, C. (2016). Fe3O4/BSA particles induce osteogenic differentiation of mesenchymal stem cells under static magnetic field.*Acta biomaterialia, 46* , 141-150.

Joshi, N., & Grinstaff, M. (2008). Applications of dendrimers in tissue engineering. *Current topics in medicinal chemistry, 8* (14), 1225-1236.

Kandpal, N., Sah, N., Loshali, R., Joshi, R., & Prasad, J. (2014). Co-precipitation method of synthesis and characterization of iron oxide nanoparticles.

Kesharwani, P., Gajbhiye, V., K Tekade, R., & K Jain, N. (2011). Evaluation of dendrimer safety and efficacy through cell line studies. *Current drug targets, 12* (10), 1478-1497.

Kesharwani, P., Tekade, R. K., Gajbhiye, V., Jain, K., & Jain, N. K. (2011). Cancer targeting potential of some ligand-anchored poly (propylene imine) dendrimers: a comparison. *Nanomedicine: Nanotechnology, Biology and Medicine, 7* (3), 295-304.

Kesharwani, P., Tekade, R. K., & Jain, N. K. (2015). Dendrimer generational nomenclature: the need to harmonize. *Drug Discovery Today, 20* (5), 497.

Khodadust, R., Unsoy, G., Yalcın, S., Gunduz, G., & Gunduz, U. (2013). PAMAM dendrimer-coated iron oxide nanoparticles: synthesis and characterization of different generations.*Journal of nanoparticle research, 15* (3), 1488.

Klajnert, B., & Bryszewska, M. (2001). Dendrimers: properties and applications. *Acta biochimica polonica, 48* (1), 199-208.

Koehler, F. M., Rossier, M., Waelle, M., Athanassiou, E. K., Limbach, L. K., Grass, R. N., . . . Stark, W. J. (2009). Magnetic EDTA: coupling heavy metal chelators to metal nanomagnets for rapid removal of cadmium, lead and copper from contaminated water. *Chemical Communications* (32), 4862-4864.

Kohli, N., Ho, S., Brown, S. J., Sawadkar, P., Sharma, V., Snow, M., & García-Gareta, E. (2018). Bone remodelling in vitro: Where are we headed?-A review on the current understanding of mimicking physiological bone remodelling and inflammation in vitro and the future strategies for testing biomaterials in vitro. *Bone* .

Liu, H., Guo, J., Jin, L., Yang, W., & Wang, C. (2008). Fabrication and functionalization of dendritic poly (amidoamine)-immobilized magnetic polymer composite microspheres. *The Journal of Physical Chemistry B, 112* (11), 3315-3321.

Marinin, A. (2012). Synthesis and characterization of superparamagnetic iron oxide nanoparticles coated with silica.

Mascolo, M. C., Pei, Y., & Ring, T. A. (2013). Room temperature co-precipitation synthesis of magnetite nanoparticles in a large pH window with different bases. *Materials, 6* (12), 5549-5567.

Miron, R., & Zhang, Y. (2012). Osteoinduction: a review of old concepts with new standards. *Journal of dental research, 91* (8), 736-744.

Ng, J., Spiller, K., Bernhard, J., & Vunjak-Novakovic, G. (2017). Biomimetic approaches for bone tissue engineering. *Tissue Engineering Part B: Reviews, 23* (5), 480-493.

Pan, B., Cui, D., Sheng, Y., Ozkan, C., Gao, F., He, R., . . . Huang, T. (2007). Dendrimer-modified magnetic nanoparticles enhance efficiency of gene delivery system. *Cancer research, 67* (17), 8156-8163.

Polo-Corrales, L., Latorre-Esteves, M., & Ramirez-Vick, J. E. (2014). Scaffold design for bone regeneration. *Journal of nanoscience and nanotechnology, 14* (1), 15-56.

POURIANAZAR, N. T. (2016). *TARGETED DELIVERY OF CPG-OLIGODEOXYNUCLEOTIDE TO BREAST CANCER CELLS BY POLY-AMIDOAMINE DENDRIMER-MODIFIED MAGNETIC NANOPARTICLES.* MIDDLE EAST TECHNICAL UNIVERSITY.

Ren, K., Wang, Y., Sun, T., Yue, W., & Zhang, H. (2017). Electrospun PCL/gelatin composite nanofiber structures for effective guided bone regeneration membranes. *Materials Science and Engineering: C, 78* , 324-332.

Robbins, S., Lauryssen, C., & Songer, M. N. (2017). Use of nanocrystalline hydroxyapatite with autologous BMA and local bone in the lumbar spine: a retrospective CT analysis of posterolateral fusion results. *Clinical spine surgery, 30* (3), E192.

Souza, T., Ciminelli, V., & Mohallem, N. (2016). *A comparison of TEM and DLS methods to characterize size distribution of ceramic nanoparticles.* Paper presented at the Journal of Physics: Conference Series.

Stevens, B., Yang, Y., Mohandas, A., Stucker, B., & Nguyen, K. T. (2008). A review of materials, fabrication methods, and strategies used to enhance bone regeneration in engineered bone tissues. *Journal of Biomedical Materials Research Part B: Applied Biomaterials, 85* (2), 573-582.

Tajabadi, M., Khosroshahi, M. E., & Bonakdar, S. (2013). An efficient method of SPION synthesis coated with third generation PAMAM dendrimer. *Colloids and Surfaces A: Physicochemical and Engineering Aspects, 431* , 18-26.

Tsao, Y.-T., Huang, Y.-J., Wu, H.-H., Liu, Y.-A., Liu, Y.-S., & Lee, O. K. (2017). Osteocalcin mediates biomineralization during osteogenic maturation in human mesenchymal stromal cells. *International journal of molecular sciences, 18* (1), 159.

Uzun, K., Çevik, E., Şenel, M., Sözeri, H., Baykal, A., Abasıyanık, M., & Toprak, M. (2010). Covalent immobilization of invertase on PAMAM-dendrimer modified superparamagnetic iron oxide nanoparticles. *Journal of nanoparticle research, 12* (8), 3057-3067.

Wang, R., Wu, H., Yang, Y., & Song, M. (2016). Effects of electromagnetic fields on osteoporosis: a systematic literature review. *Electromagnetic biology and medicine, 35* (4), 384-390.

Xia, Y., Chen, H., Zhao, Y., Zhang, F., Li, X., Wang, L., . . . Gu, N. (2019). Novel magnetic calcium phosphate-stem cell construct with magnetic field enhances osteogenic differentiation and bone tissue engineering. *Materials Science and Engineering: C, 98* , 30-41.

Xia, Y., Sun, J., Zhao, L., Zhang, F., Liang, X.-J., Guo, Y., . . . Xu, H. H. (2018). Magnetic field and nano-scaffolds with stem cells to enhance bone regeneration.*Biomaterials, 183* , 151-170.

Yen, C.-H., Lien, H.-L., Chung, J.-S., & Yeh, H.-D. (2017). Adsorption of precious metals in water by dendrimer modified magnetic nanoparticles. *Journal of hazardous materials, 322* , 215-222.

Zhao, X., Kim, J., Cezar, C. A., Huebsch, N., Lee, K., Bouhadir, K., & Mooney, D. J. (2011). Active scaffolds for on-demand drug and cell delivery. *Proceedings of the National Academy of Sciences, 108* (1), 67-72.

Zhu, R., Jiang, W., Pu, Y., Luo, K., Wu, Y., He, B., & Gu, Z. (2011). Functionalization of magnetic nanoparticles with peptide dendrimers. *Journal of Materials Chemistry, 21* (14), 5464-5474.

Figure captions

Fig. 1. The schematic representation of the synthesis reaction of G3- SPION.

Fig. 2. (a) TEM photograph and size distribution histogram of G3–SPIONs. (b) DLS and (c) Zeta potential measurements of the G3–SPIONs.

Fig. 3. (a) FTIR spectrum of the neat SPIONs, APTES, G1, G2, and G3 grafted SPIONs. (b) VSM result of SPIONs and G3-SPIONs.

Fig. 4. SEM image and histogram of nanofibers (a) PCL (b) G3-SPION-PCL.

Fig. 5. (a) The MTT cell viability and (b) DAPI staining of ADMSCs cultured on the PCL and G3-SPION-PCL scaffolds.

Fig. 6. Biochemical analyses of differentiated cells on TCP, PCL, and G3-SPION-PCL scaffolds under OM or/and PEMF condition; (a) ALP activity, (b) Calcium content. (Data are expressed as means ± SD and p-Value of less than 0.05 were interpreted as being significant, showing as one asterisk.), (c) Morphological analyses of ADMSCs during osteogenic differentiation on G3-SPION-PCL scaffold after 1 and 14 days.

Fig 7. Relative expression of OC, Col 1, and Runx2 on day 14 for ADMSCs cultured on the G3-SPION-PCL in the presence of OM and,or PEMF.

Table 1. The primer sequences used in RT-PCR to quantify the osteogenic differentiation.

Gene	Forward primer sequence	Reverse primer sequence
Osteocalcin (OC)	5'-GCAAAGGTGCAGCCTTTGTG	5'-GGCTCCCAGCCATTGATACAG
Runt-related transcription factor 2 (Runx2)	5'-GCCTTCAAGGTGGTAGCC	5'-CGTTACCCGCCATGACAGTA
Collagen type 1 (Col1)	5'-TGGAGCAAGAGGCGAGAG	5'-CACCAGCATCACCCTTAGC
β2M	5'-ATGCCTGCCGTGTGAAC	5'-ATCTTCAAACCTCCATGATG

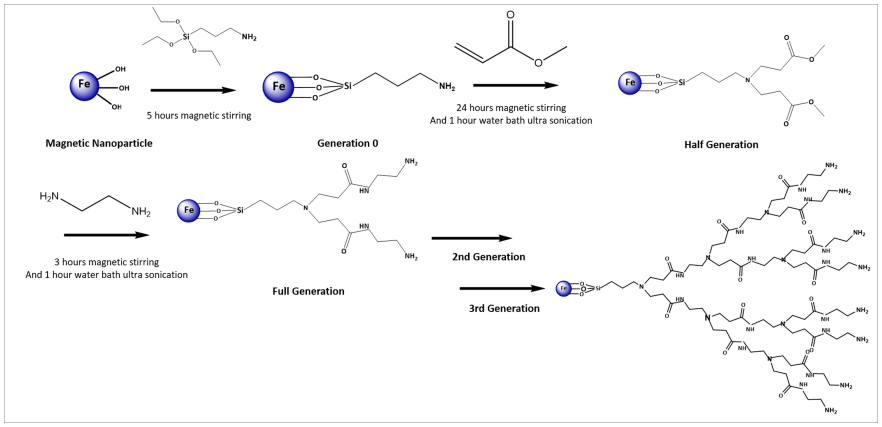

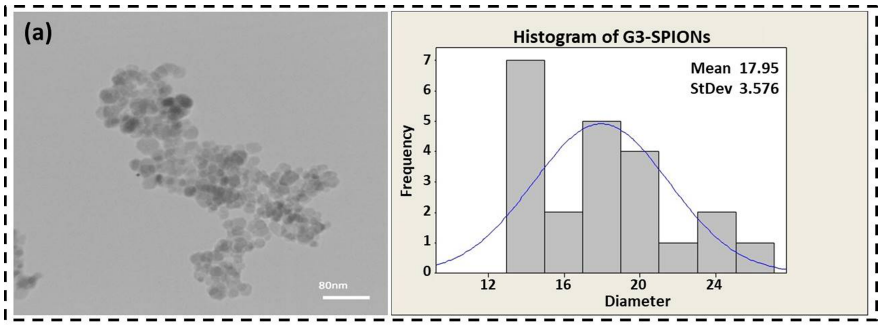

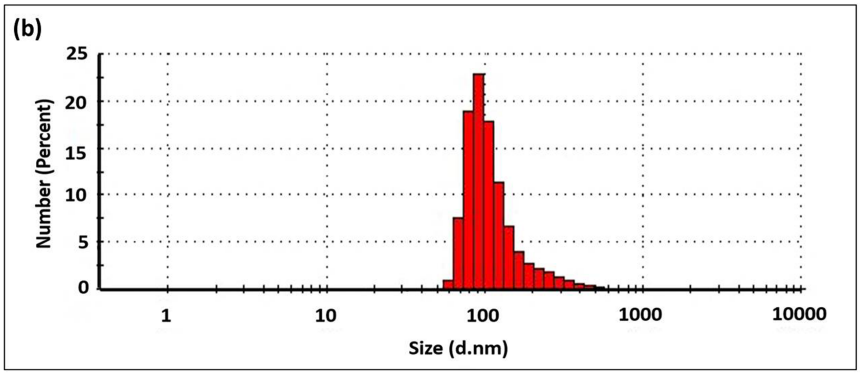

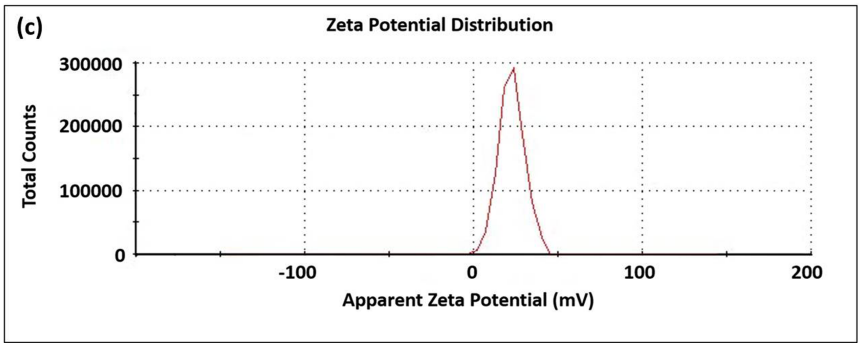

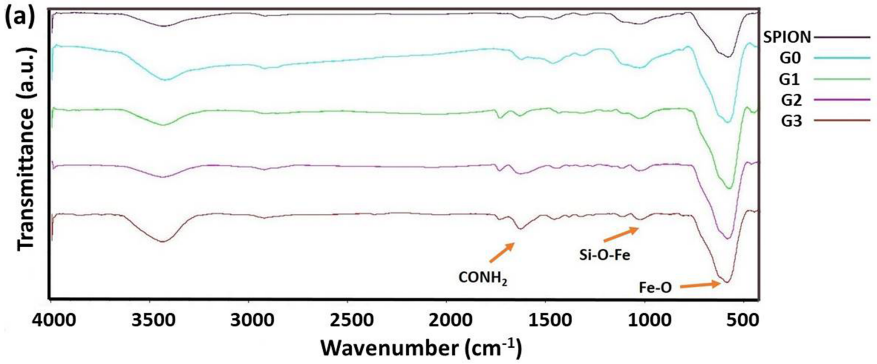

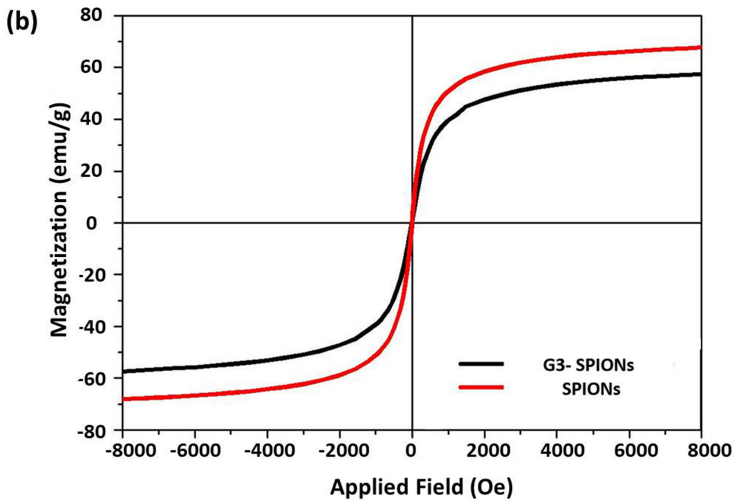

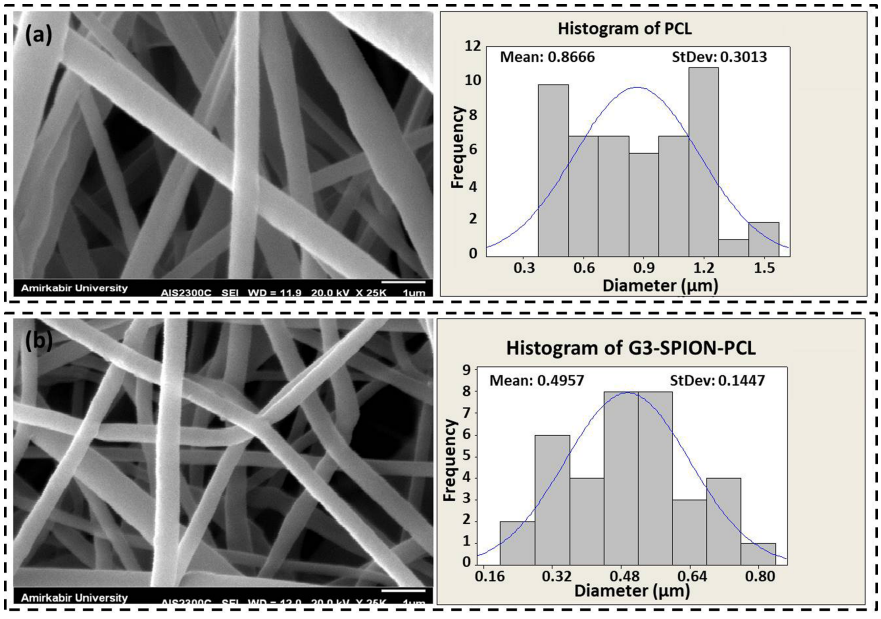

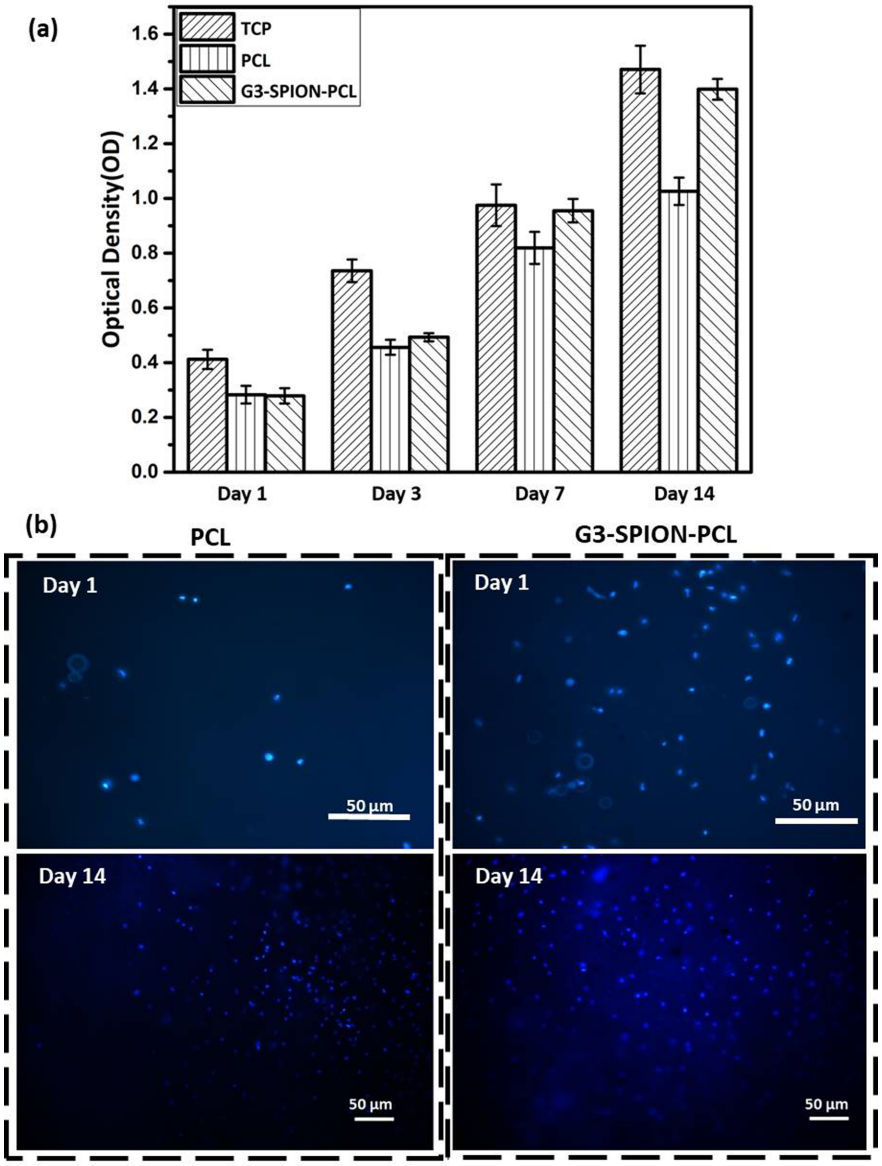

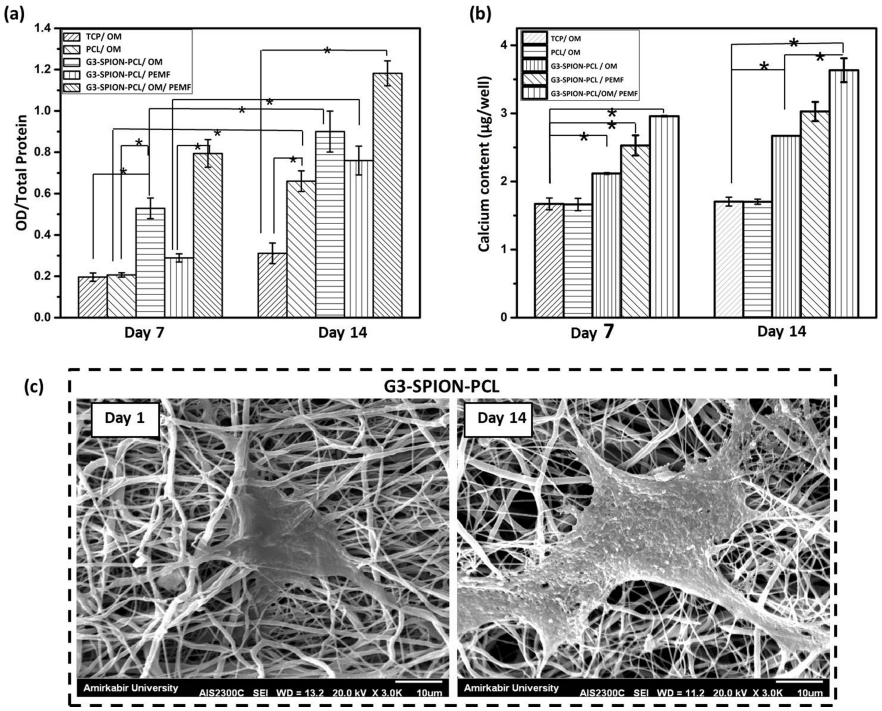

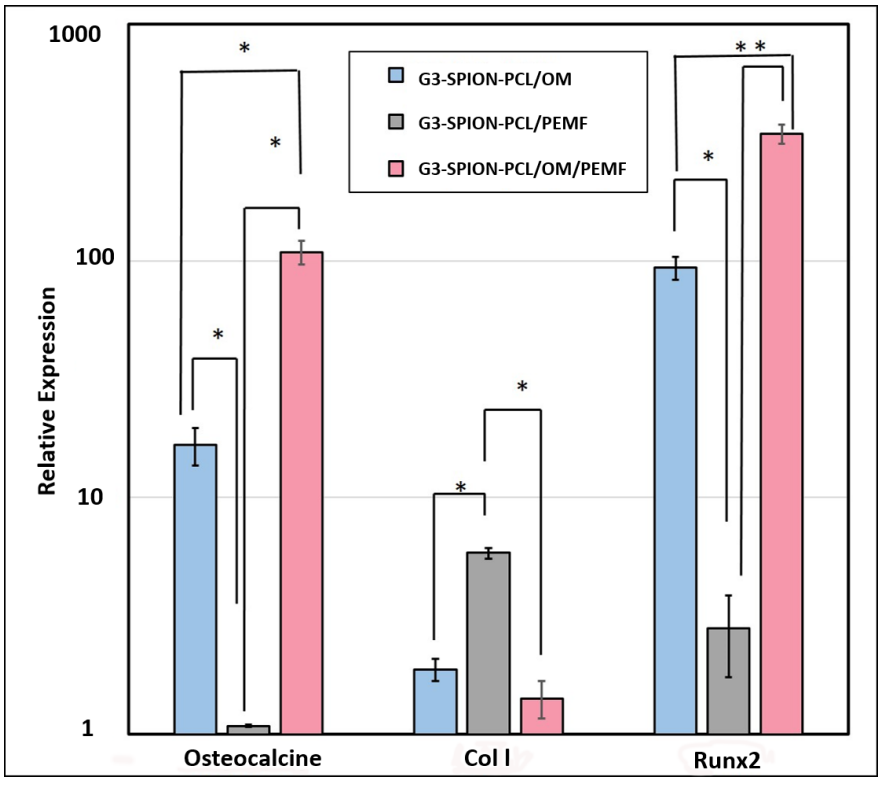

Hosted file

Table .docx available at https://authorea.com/users/358612/articles/480713-study-of-osteogenic-potential-of-electrospun-pcl-incorporated-by-dendrimerized-superparamagnetic-nanoparticles-as-a-bone-tissue-engineering-scaffold